Large Eddy Simulation of Smooth- and Rough-wall Channel Flow – Description of Implementation

Namiko Saito, Michio Inoue, Dale I. Pullin

The set of code in the enclosed .zip file computes rough-wall turbulent channel flow. This brief note summarizes what is implemented in the code. For a more complete description of the theories and discussions of the results, readers are referred to the work by Saito *et al.*[9]. Please also refer to the work by Chung & Pullin[1], who discussed smooth channel flows and provided a comprehensive explanation of the models used in our large eddy simulations (LES). Inoue & Pullin[4] studied smooth flat plate turbulent boundary layer flows using this method and Inoue[3] described the numerical techniques implemented in the present code.

Our LES employs the stretched vortex subgrid-scale (SGS) model and a wall model and has allowed for the simulation of long channel flows up to 128δ in streamwise extent, where δ is the perpendicular distance from the wall to the channel centerline. The outer LES solves the Navier-Stokes equations for the velocity field where the sub-grid components of the field are incorporated in the form of SGS stresses. The outer LES exchanges information with the wall model at each time step to create a coupling between the two. The use of the wall model circumvents the high computational costs associated with resolving the near-wall anisotropy and fine-scaled motions, thus eliminating the majority of grid points needed for wall-resolved high Reynolds number computations. We attain friction Reynolds numbers up to $Re_\tau = 2 \times 10^8$ as a result. Note that at these Reynolds numbers, roughness corrections are crucial and hence we embed such corrective terms within our wall model as nominal analytical expressions. The present code utilizes Colebrook's empirical formula and this is what gives rise to the semi-empirical nature of our results. Note that the model is compatible with alternative roughness formulae.

The present discussion addresses three key elements of our simulation: solving the Navier-Stokes equations, the stretched vortex SGS model and the roughness-corrected wall model. These are followed by introducing some of our results for rough-wall turbulent channel flow simulations.

1 Solving Navier-Stokes equation

In the outer LES, we solve the Navier-Stokes equations (1) under the assumption that the fluid is Newtonian, viscous and incompressible.

$$\begin{aligned} \frac{\partial \mathbf{u}}{\partial t} + \mathbf{u} \cdot \nabla \mathbf{u} &= -\nabla p + \frac{1}{Re} \nabla^2 \mathbf{u} \\ \nabla \cdot \mathbf{u} &= 0 \end{aligned} \tag{1}$$

Here, bold-face denotes vectors. The velocity vector and pressure are denoted by $\mathbf{u}$ and p respectively. As introduced in Perot[7], this set of equations can be discretized and set in matrix form,

$$\begin{bmatrix} \mathbf{A} & \mathbf{G} \\ \mathbf{D} & \mathbf{0} \end{bmatrix} \begin{bmatrix} \mathbf{u}^{n+1} \\ p^{n+1} \end{bmatrix} = \begin{bmatrix} \mathbf{r}^n \\ 0 \end{bmatrix} + \begin{bmatrix} bc_1 \\ bc_2 \end{bmatrix}, \tag{2}$$

where the current time step is denoted by n. The operators $\mathbf{A}$, $\mathbf{D}$ and $\mathbf{G}$ are respectively the advection-diffusion, divergence and gradient operators. Denoted by $\mathbf{r}^n$ is the explicit term on the right-hand-side of the momentum equations. The specific forms for these operators depend on the discretization schemes used in the simulation. The first boundary condition bc_1 is imposed on the momentum equation and the second boundary condition bc_2 is imposed on the continuity equation.

Through block LU factorization and first-order approximation of the advection-diffusion operator, the matrix system (2) reduces down to the following system of equations,

$$\begin{aligned} \mathbf{A}\ \mathbf{u}_*^{n+1} &= \mathbf{r}^n + \beta_m bc_1, \\ dt(\alpha_m + \beta_m)\mathbf{D}\ \mathbf{G}p &= (\mathbf{D}\ \mathbf{u}_*^{n+1} + bc_2), \\ \mathbf{u}^{n+1} &= \mathbf{u}_*^{n+1} - dt(\alpha_m + \beta_m)\mathbf{G}p, \end{aligned} \tag{3}$$

where

$$\begin{aligned} \mathbf{A} &= \mathbf{I} - \frac{\beta_m dt}{Re}\mathbf{L}, \\ \mathbf{r}^n &= dt\left[-\gamma_m \mathbf{N}\ \mathbf{u}^n - \xi_m \mathbf{N}\ \mathbf{u}^{n-1} + \alpha_m(\mathbf{L}\ \mathbf{u}^n + bc_1^n)\right]. \end{aligned}$$

Here, the matrix $\mathbf{I}$ is the identity matrix and $\mathbf{L}$ is the Laplacian operator. The subscript m denotes the index that follows the fractional steps. The values of coefficients, α_m, β_m, γ_m and ξ_m are associated with the low-storage third-order Runge-Kutta method of Spalart[10]. The spatial discretization employs a fourth-order finite difference method on a staggered grid in the streamwise (x) and wall-normal (y) directions and a pseudo-spectral method is applied in the spanwise direction (z).

The channel has two periodic directions, streamwise and spanwise, resulting in the periodic boundary conditions at these boundaries. The wall boundaries

are smooth or have varying degrees of roughness with their effects imposed on the outer LES by way of the wall model. This wall model calculates and provides a Dirichlet-type velocity boundary condition at a lifted 'virtual' wall. This then forms the complete set of boundary information for the outer LES calculation to take place, with details of this calculation to follow.

2 Stretched vortex SGS model

The stretched-vortex model is a structural SGS model that is designed to represent the statistical effect of subgrid motion by using information from resolved scale motions[6]. It is assumed that the subgrid vorticity in each cell comprises a superposition of stretched vortices, each unidirectional and of 'cylindrical' type. This arrangement is formulated in the vortex-fixed frame of reference and when converted to the lab-fixed frame, the distribution of orientations of the vortex structures forms a probability density function (PDF) which reflects the local turbulence anisotropy (Pullin[2]). Building on another assumption that the ensemble dynamics of subgrid scale motion are dominated by a vortex aligned with a unit vector e^v, which forms a delta-function PDF, the subgrid stress tensor $T_{ij} = \widetilde{u_i u_j} - \widetilde{u}_i \widetilde{u}_j$ is given by (Pullin & Saffman[8]; Chung & Pullin[1])

$$T_{ij} = \left(\delta_{ij} - e_i^v e_j^v\right) K. \tag{4}$$

In (4), the subgrid kinetic energy K is expressed in (5) with a group constant $\mathcal{K}_0'$ and an incomplete gamma function,

$$K \quad = \quad \frac{1}{2}\mathcal{K}_0' \Gamma[-\frac{1}{3}, \kappa_c^2], \text{ where } \Gamma[s,t] = \int_t^\infty u^{s-1} \exp(-u) du, \tag{5}$$

where $\mathcal{K}_0' = \mathcal{K}_0 \epsilon^{2/3} \lambda_v^{2/3}$, $\lambda_v = (2\nu/3|\overline{a}|)^{1/2}$ and $\kappa_c = k_c \lambda_v$. The approximation of $\Gamma[s,t]$ and the evaluation of $\mathcal{K}_0'$ are given in Chung & Pullin[1].

3 Wall model with roughness

Located between the physical wall and the first grid cell, the virtual wall is where the wall model defines the slip velocity for use by the outer LES via a two stage calculation process. First, given information from the outer LES, an ordinary differential equation (ODE) is solved numerically in order to dynamically and locally determine the friction velocity $u_\tau(x,z,t)$. Second, the slip velocity is evaluated at the lifted virtual wall at $h_0 = 0.18\Delta y$, where Δy is the wall-normal grid size. Since this slip velocity boundary condition is the only feedback mechanism for near-wall information to reach the outer flow, no explicit corrections for roughness are required at each grid point in the outer LES calculation.

The ODE described above (6) is derived from the streamwise momentum equation after wall-parallel filtering of the streamwise momentum equation followed by wall-normal averaging from the wall to the first computational grid

cell[1, 9]. The roughness effect, appearing in the denominator, is based on the Colebrook formula $\Delta U^+ = -\kappa^{-1}\log\left(1+0.26k^+_{s\infty}\right)$, where $k_{s\infty}$ is the equivalent sand roughness [5]. Note that the smooth-wall condition is recovered simply by setting the equivalent sand roughness to zero. The time-integration of this ODE to solve for $u_\tau(x,z,t)$ is performed side-by-side with the integration of the Navier-Stokes equation under the same low-storage third-order semi-implicit Runge-Kutta scheme of Spalart[10]).

$$\frac{du_\tau}{dt} = \frac{-\left.\frac{\partial\widetilde{uu}}{\partial x}\right|_h - \left.\frac{\partial\widetilde{uw}}{\partial z}\right|_h - \left.\frac{\partial\widetilde{P}}{\partial x}\right|_h - \frac{1}{h}\widetilde{uv}\mid_h + \frac{\nu}{h}\left.\frac{\partial\widetilde{u}}{\partial y}\right|_h - \frac{1}{h}u_\tau^2}{\frac{\widetilde{u}\mid_h}{u_\tau} - k^+_{s\infty}\frac{\partial\Delta U^+}{\partial k^+_{s\infty}}}. \tag{6}$$

Both the dynamically and locally calculated friction velocity u_τ from (6) as well as the Kármán constant $\mathcal{K}_1(x,z,t)$, calculated in the outer LES[1, 4, 9], are required for the evaluation of the roughness corrected slip velocity according to the following expression:

$$\widetilde{u}\mid_{h_0} = u_\tau\left(\frac{1}{\mathcal{K}_1}\log\left(h_0^+\right) + B - \frac{1}{\mathcal{K}_1}\log\left(1+0.26\,k^+_{s\infty}\right)\right). \tag{7}$$

4 Results

The mean velocity profiles obtained by running a series of simulations are shown in Figure 1 . Both Reynolds number and roughness level are varied, with results shown here similar but covering a smaller range of $k^+_{s\infty}$ compared to those in Saito *et al.*[9]. A characteristic of rough-walled turbulence is the presence of a velocity deficit due to the roughness induced loss of momentum at the wall, where higher roughness generates a larger deficit. This signature behavior is noted in the figure. Worth mentioning is the consistency in the agreement between LES results and the empirical log-law across the wide array of test conditions. Please refer to the original paper for in depth discussion of these and other results.

References

[1] D. Chung and D. I. Pullin. Large-eddy simulation and wall-modeling of turbulent channel flow. *Journal of Fluid Mechanics*, 631:281–309, 2009.

[2] D.I. Pullin D.I. and P.G. Saffman. Vortex dynamics in turbulence. *Ann. Rev. Fluid Mech.* , **30**:31–51, 1997.

[3] M Inoue. *Large-Eddy Simulation of the Flat-plate Turbulent Boundary Layer at High Reynolds numbers*. PhD thesis, California Institute of Technology, 2012.

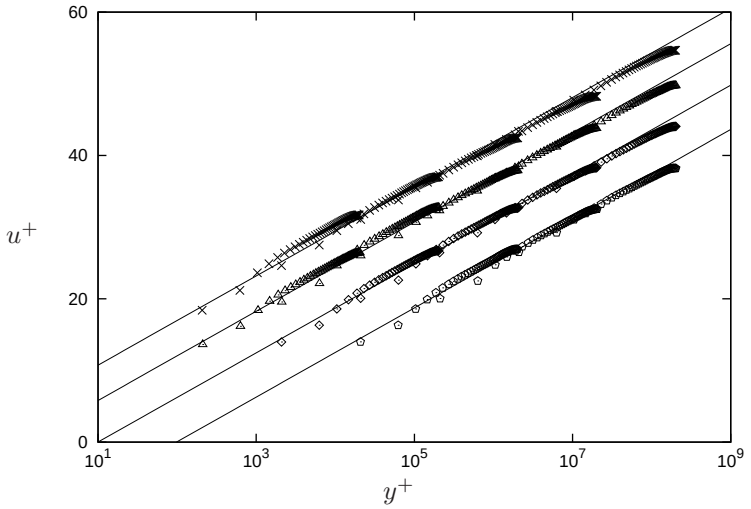

Figure 1: Mean velocity profiles. Open symbols, LES results $\times$: $\epsilon Re_\tau = 0$, $\triangle$: $\epsilon Re_\tau = 20$, $\diamond$: $\epsilon Re_\tau = 200$, $\pentagon$: $\epsilon Re_\tau = 2000$. Solid lines, empirical log law with Colebrook's formula.

[4] M. Inoue and D. I. Pullin. Large-eddy simulation of the zero-pressure-gradient turbulent boundary layer up to $Re_\theta = \mathcal{O}(10^{12})$. *Journal of Fluid Mechanics*, pages 1–27, September 2011.

[5] J. Jiménez. Turbulent flows over rough walls. *Annual Review of Fluid Mechanics*, 36(1):173–196, January 2004.

[6] A. Misra and D. I. Pullin. A vortex-based subgrid stress model for large-eddy simulation. *Phys. Fluids*, 9:2443–2454, 1997.

[7] J.B. Perot. An analysis of the fractional step method. *Journal of Computational Physics*, 108(1):51–58, 1993.

[8] D.I Pullin and P.G. Saffman. Reynolds stresses and one-dimensional spectra for vortex models of homogeneous anisotropic turbulence. *Phys Fluids* , **6** :1787, 1994.

[9] Namiko Saito, Dale I Pullin, and Michio Inoue. Large eddy simulation of smooth-wall, transitional and fully rough-wall channel flow. *Physics of Fluids*, 24(7):075103, 2012.

[10] P. R. Spalart, R. D. Moser, and M. M. Rogers. Spectral methods for the Navier–Stokes equations with one infinite and two periodic directions. *J. Comp. Phys.*, 96:297–324, 1991.